Flash method and Bayesian inference for measurement of thermophysical fields

Marie-Marthe Groz, A. Sommier, E. Abisset-Chavanne, J. Batsale, C. Pradere

Flash Method and Bayesian inference for measurement of thermophysical fields

M.M. Groz[a]*, A. Sommier[a], E. Abisset-Chavanne[a], J.C. Batsale[a] and C. Pradere[a]

[a] I2M UMR CNRS 5295, Esplanade des Arts et Métiers, 33405 Talence Cedex, France.

Abstract

In this paper, a method based on Bayesian inference is proposed to conjointly estimate the following two fields of thermophysical parameters. The first is a thermal characteristic time directly linked to the thermal diffusivity and the thickness, whereas the second is the Biot number, which is directly linked to the heat loss and thermal conductivity. This method is robust to noise and leads to very good estimations of the parameters, with an algorithm that is very fast and less time consuming than a classical minimization method. At the end of the study, a setup and a methodology are also presented to estimate the average value of the thermal conductivity of an unknown material.

*Corresponding author: marie-marthe.groz@u-bordeaux.fr

1 Introduction

Thermal diffusivity is one of the main parameters in the thermal characterization of materials. The method proposed by Parker [1] is one of the oldest thermal methods used for the characterization of diffusion by rear face flash. The hypotheses considered in Parker's method are that the excitation flux is uniform over the entire surface and is of short duration (Dirac-type excitation in time). The material is also considered adiabatic. Under these conditions, the maximum sensitivity to thermal dispersion is reached at the half-rise time $t_{1/2}$ of the normalized thermogram. Parker's method is still widely used because of its implementation simplicity and its large application domain because it can be used for insulators as well as for conductors. However, the assumptions that it requires are not always realistic; in particular, adiabatic boundary conditions are rarely verified. Indeed, the conductive heat losses at material surfaces are rarely negligible. Since this method was presented, several methods were subsequently proposed to take into account the thermal losses for diffusivity estimation. Among them, the method proposed by Balageas [2] was to focus the study near the time origin, where the influence of heat loss is low. Other methods proposed by Degiovanni *et al.* use particular points of the thermogram during the rising time or the temporal moments between two points to estimate the diffusivity [3, 4, 5]. Another example is the method of partial times with convective losses proposed by Degiovanni [6] or the approach of asymptotic expansions proposed by Mourand [7]. Most of these methods use particular points or areas of the thermograms to estimate the diffusivity. Other works proposed estimating the thermal diffusivity with whole thermograms using least-squares methods by minimizing the residual composed of the norm of the difference between the measured data and the theoretical model [8, 9, 10, 11]. Most recently, a method was developed [12, 13] to calculate the thermal diffusivity as well as a global estimation of the heat losses. These parameters are estimated through the Biot numbers and calculated from the ratio between the integrals of the complete temperature trends of the two faces. One of the difficulties of all these methods is their sensitivity to noise level. During the last two decades, Bayesian methodologies were developed [14, 15], which have the advantage of being minimally sensitive to noise. In these works, the Markov chain Monte Carlo method (MCMC) is used.

In this paper, a method based on Bayesian inference is proposed to locally and conjointly estimate the two parameters on each point of the material with whole thermograms without using the MCMC methods but with the generation of a base that represents the physical model. This method is compared to the classical minimizations method using least squares, and the performances are compared, particularly on the estimation precision and the time computation of the algorithm. At the end of this work, a methodology is also proposed to quantify the average value of the thermal conductivity of a material.

2 Methodology for the simultaneous estimation of the heat loss and the diffusivity

2.1 Experimental setup

Originally, the experimental setup proposed by Parker was made with a thermocouple. Now, with the advance of the technology, a classical rear face flash system is associated with an IR camera. The setup used in this paper is presented in figure 1.

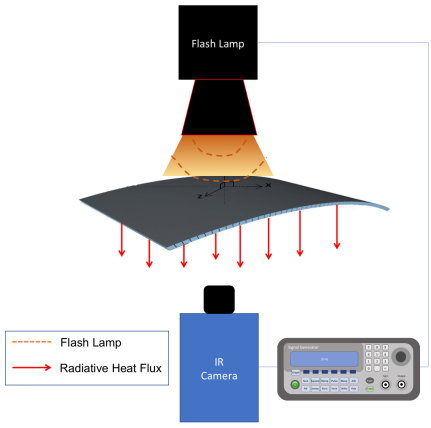

Fig. 1: Schema of the experimental setup.

The flash lamp comes from Uniblitz and has an energy E of 1600 J. The lamp is synchronized with the IR camera by using an analogical TTL link to perform a pretrigger mode before the flash. The IR camera is an MCT longwave ($\lambda = 9\text{-}11\mu$m) FLIR SC7600 with a matrix sensor of 320×256 pixels and a pitch of 30×30 μm^2. With the lenses used and the sample distance, the resulting spatial resolution was 280×280 μm^2 per pixel.

2.2 Direct model

In the rear flash experiment, the sample is subjected to a heat pulse of energy Q_0 (J·m^{-2}) on its front face $z = 0$. The convective losses are modeled by the heat transfer coefficients h_0 and h_e (W·m^{-2}·K^{-1}) for the front and rear faces, respectively, as illustrated by figure 2.

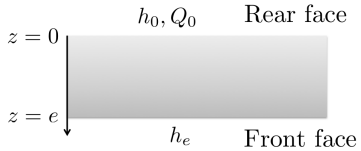

Fig. 2: Schema of the material.

The governing equations [16] are then given by:

$$\begin{cases} \dfrac{\partial T(z,t)}{\partial t} = a\dfrac{\partial^2 T(z,t)}{\partial z^2} \\ -\lambda\dfrac{\partial T(z,t)}{\partial z}\Big|_{z=0} = Q_0\delta(t) - h_0 T(0,t) \\ -\lambda\dfrac{\partial T(z,t)}{\partial z}\Big|_{z=e} = h_e T(e,t) \end{cases} \tag{1}$$

where a is the diffusivity coefficient ($m^2 \cdot s^{-1}$), λ is the thermal conductivity ($W \cdot m^{-1} \cdot K^{-1}$) and e the thickness of the material (m).

In the Laplace domain, equation 1 takes the following form:

$$\begin{cases} p\,\theta(z,p) = a\dfrac{d^2\theta(z,p)}{dz^2} \\ -\lambda\dfrac{d\theta(z,p)}{dz}\Big|_{z=0} = Q_0 - h_0\theta(0,p) \\ -\lambda\dfrac{d\theta(z,p)}{dz}\Big|_{z=e} = h_e\theta(e,p) \end{cases} \tag{2}$$

As presented in equation 3, we can introduce the τ (s) parameter and the dimensionless Biot numbers for the rear face Bi_0 and the front face Bi_e:

$$\tau = \frac{e^2}{a} \;\; ; \;\; Bi_0 = \frac{h_0 e}{\lambda} \;\; ; \;\; Bi_e = \frac{h_e e}{\lambda}, \tag{3}$$

Equation 2 can easily be solved in terms of the rear face Laplace temperature:

$$\theta(e,p) = \frac{e}{\lambda}\frac{2Q_0\sqrt{p\tau}e^{-\sqrt{p\tau}}}{\left(Bi_0+\sqrt{p\tau}\right)\left(Bi_e+\sqrt{p\tau}\right) - \left(\sqrt{p\tau}-Bi_0\right)\left(\sqrt{p\tau}-Bi_e\right)e^{-2\sqrt{p\tau}}} \tag{4}$$

In this paper, the heat losses are assumed to be identical on the front and rear faces; therefore, $Bi_0 = Bi_e = Bi$. As $\lambda = a\rho C_p$, where ρ ($kg \cdot m^{-3}$) and C_p ($J \cdot K^{-1} \cdot kg^{-1}$) are the density and specific heat of the material, respectively, equation 4 can be simplified and written as:

$$\theta(e,p) = \frac{2Q_0}{e\rho C_p}\frac{\tau\sqrt{p\tau}e^{-\sqrt{p\tau}}}{\left(Bi+\sqrt{p\tau}\right)^2 - \left(\sqrt{p\tau}-Bi\right)^2 e^{-2\sqrt{p\tau}}} \tag{5}$$

A numerical inverse Laplace transform can then be performed on equation 5 by using the Stehfest algorithm [17, 16] to calculate the temperature in the temporal domain.

In the flash method, the quantity of energy Q_0 is hard to quantify because it is not directly related to the light energy quantity that is radiated by the flash lamp. Actually, the energy received by the sample is also a function of the optical properties as the absorption of the sample. To

remove this parameter, the temperature is normalized. The thermogram is then normalized by the maximum value of the temperature, which leads to a temperature variation between 0 and 1. Thanks to this normalization, the temperature is only dependent on the Biot number and the parameter τ.

2.3 Sensitivity study with respect to the parameters

In this paper, the objective is the estimation of both the diffusivity a and the heat losses h on a sample. However, the parameters τ and Bi have the advantage of being more universal. Indeed, a fixed value of τ can correspond to different couples (a, e) of diffusivities and thicknesses. Therefore, the estimation of the parameter τ enables the estimation of the diffusivity a if the thickness e is known, or inversely, the estimation of the thickness e if the diffusivity a is known. Likewise, a fixed Biot number can correspond to a large number of couples (h, e, λ), and the estimation of each of these parameters can be made. In particular, if the thickness e is known, a characteristic length corresponding to a convecto-conductive ratio can be estimated. Thus, throughout the rest of the paper, the study will be conducted with the parameters τ and Bi.

A sensitivity study with respect to the parameters τ and Bi is therefore performed in this part to highlight the influence of each of these parameters on the temperature. Several thermal responses are computed with the help of equation 5 by varying these parameters. Figure 3.a presents the normalized thermograms for $Bi = 0.2$ and for different τ between 10 and 100, whereas Figure 3.b illustrates the normalized thermograms for $\tau = 100$ and for Bi varying between 0 and 2. The study of the influence of each of the two parameters (τ, Bi) is performed with the help of the partial derivatives of the thermal responses with respect to these two parameters. Figure 3.c illustrates the partial derivatives $\partial T/\partial \tau$ of each of the thermograms of Figure 3.a, whereas Figure 3.d illustrates the partial derivatives $\partial T/\partial Bi$ of each of the thermograms of Figure 3.b.

For a fixed Biot number, the higher the value of τ (*i.e.* the smaller the diffusivity a for a fixed thickness), the later the maximum temperature is reached. Predictably, as concluded by Parker [1], the maximum sensitivity with respect to the τ parameter, given by the maximum of the partial derivatives illustrated in figure 3.c, is reached at the half rise time $t_{1/2}$ of each normalized thermogram (illustrated in figure 3.a).

Conversely, for a fixed parameter τ, the higher the Biot number (*i.e.* the higher the heat losses), the sooner the maximum temperature is reached. The maximum sensitivity with respect to the Biot number is reached after the rise time of the temperature. Predictably, for small values of Bi, the sensitivity of the thermal response with respect to this parameter is low, but the higher the values of Bi are, the less the influence of this parameter is negligible. To emphasize this

point, the estimation of the τ parameter with the Parker method is performed for different values of Biot numbers between 0 and 2 and for $\tau = 100$.

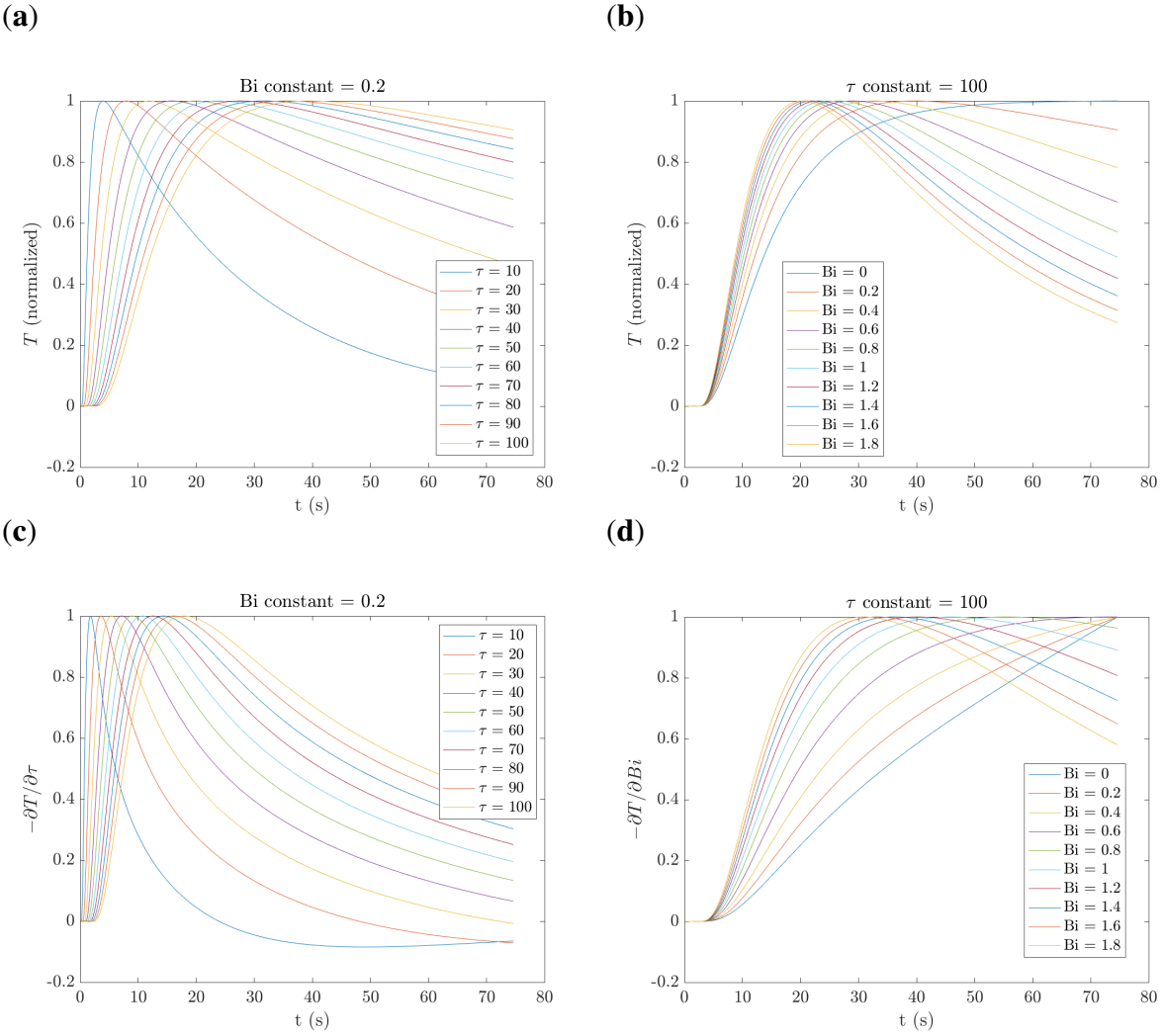

*Fig. 3: Sensitivity study with respect to the parameters τ and Bi. Normalized temperatures for **(a)** $Bi = 0.2$ constant and different values of τ and **(b)** $\tau = 100$ constant and different values of Biot number. Partial derivatives of the thermograms with respect to **(c)** the parameter τ for a fixed Biot number and **(d)** the Biot number for a fixed τ.*

The method proposed by Parker [1] consists of determining the thermal diffusivity a of the material with the help of equation 6:

$$a = 0.139\frac{e^2}{t_{1/2}}, \tag{6}$$

where a (m·s^{-2}) is the diffusivity coefficient and e (m) is the depth of the material. This equation can be written with the τ parameter as:

$$\tau = \frac{t_{1/2}}{0.139}. \tag{7}$$

The Parker estimation of the τ parameters and the absolute errors performed as percentages are illustrated in figure 4 for the different Biot numbers.

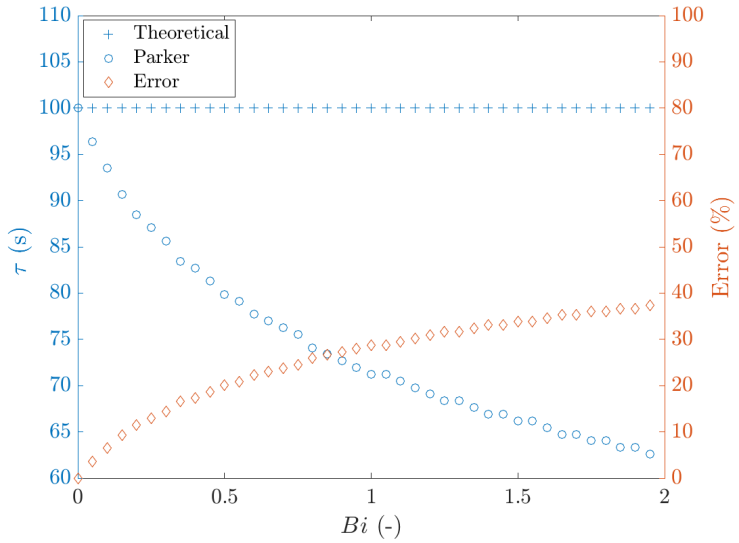

Fig. 4: Estimation of the τ parameter (diffusivities) with the Parker method for different Biot numbers (heat losses) and the corresponding absolute errors (in percentage).

τ is underestimated when Bi is a nonnull value (*i.e.* in presence of heat losses). Moreover, the higher Bi is, the higher the error performed on the estimation of τ. For $Bi = 2$, the error is almost 40%, which is nonnegligible. This result is explained by the fact that the maximum temperature is reached sooner with increasing values of Bi, and therefore, the value $t_{1/2}$ is underestimated. The estimation of the Biot number is thus required to obtain a good estimation of the τ parameter.

2.4 Estimation methodology with Bayesian inference

The method generally used for the estimation of both of the parameters is an inversion. The Levenberg-Marquardt (LM) algorithm [18] is usually computed for this problem because of its ease of implementation. However, for a large number of measures, the inversion algorithm can be time consuming. In this paper, a methodology based on Bayesian inference is proposed as an alternative and compared to LM inversion.

The problem of sample characteristics estimation can be defined in each pixel of the image as follows: knowing the measured temperature evolution $T_m(t)$ at $z = e$ (front face), determine the Biot number Bi and the parameter τ, *i.e.*, the couple $\boldsymbol{\beta} = (\tau, Bi)$.

The methodology proposed in this paper uses Bayesian inference, a probabilistic method based on the Bayes relation [19]:

$$\pi_{posterior}(\boldsymbol{\beta}|T_m(t)) = \frac{\pi(T_m(t)|\boldsymbol{\beta}) \cdot \pi_{prior}(\boldsymbol{\beta})}{\pi(T_m(t))} \tag{8}$$

- $\pi_{posterior}(\boldsymbol{\beta}|T_m(t))$ is the **posterior** probability density, *i.e.* the conditional probability of $\boldsymbol{\beta}$, given the measured temperature $T_m(t)$.
- $\pi_{prior}(\boldsymbol{\beta})$ is the **prior** density, which is the *a priori* information about $\boldsymbol{\beta}$ prior to the measurements.
- $\pi(T_m(t)|\boldsymbol{\beta})$ is the **likelihood** function, which expresses the likelihood of different temperature measurement outcomes $T_m(t)$ with $\boldsymbol{\beta}$ given.
- $\pi(T_m(t))$ is the model **evidence** or the marginal probability density of the measurements, which plays the role of a normalizing constant.

Bayesian inference is then a stochastic approach that results in a probability density function providing a probability weight to each possible variable $\boldsymbol{\beta}$. In this paper, the evidence is not considered. Indeed, even if its computation does not represent a tricky issue due to the analytical nature of the direct problem, the knowledge of the more probable $\boldsymbol{\beta}$ in each pixel, independent of the normalization, is sufficient to reconstruct the sample diffusivity and loss coefficient fields. For the prior, which allows us to account for the *a priori* knowledge of $\boldsymbol{\beta}$, only a limitation of the parametric space (τ, Bi) in the variation range of the parameters is considered to be as general as possible. The prior is taken as a uniform probability of the variation range of each parameter $[\tau_{min}, \tau_{max}]$ and $[Bi_{min}, Bi_{max}]$ with a null probability outside. Finally, in this case, the posterior probability density is directly linked to the likelihood function [20]:

$$\pi_{posterior}(\boldsymbol{\beta}|T_m(t)) \propto \pi(T_m(t)|\boldsymbol{\beta}), \boldsymbol{\beta} \in [\tau_{min}, \tau_{max}] \times [Bi_{min}, Bi_{max}] \tag{9}$$

The likelihood function $\pi(T_m(t)|\boldsymbol{\beta})$ is defined as follows:

$$\pi(T_m(t)|\boldsymbol{\beta}) \propto \exp\left(-\frac{1}{2\Gamma^2}||T_m(t) - T_r(t,\boldsymbol{\beta})||_2^2\right), \tag{10}$$

where $T_r(t,\boldsymbol{\beta})$ is the front face temperature of reference computed using the direct model defined in section 2.2 for $\boldsymbol{\beta} \in [\tau_{min}, \tau_{max}] \times [Bi_{min}, Bi_{max}]$, and $T_m(t)$ is the measured front face temperature at each pixel. Γ is the standart deviation and is set at 1 in this paper.

In this case, as the forward problem is analytical and few parameters are considered, the likelihood function is built by directly sampling the discretized parametric space (τ, Bi). This

allows us to not have to rely on Markov chain Monte Carlo methods, which are commonly used when the large computation time of the forward problem prevents the exploration of the entire parameter space [20, 21, 22, 23].

3 Presentation and study of the method

3.1 Application on numerical examples

In this section, the thermograms are numerically computed for different (τ, Bi) to evaluate the performance of the proposed Bayesian methodology. To study the Bayesian method, three thermal responses are studied with different couples of parameters (τ, Bi):

- T_1, with $\tau = 100$ s and $Bi = 0.1$.
- T_2, with $\tau = 100$ s and $Bi = 0.5$.
- T_3, with $\tau = 50$ s and $Bi = 1$.

White noise is added to each of these temperatures to simulate a real thermogram. These thermal responses are illustrated in figure 5.a for a low noise level (SNR = 200) and in figure 5.b for a high noise level (SNR = 20).

(a) **(b)**

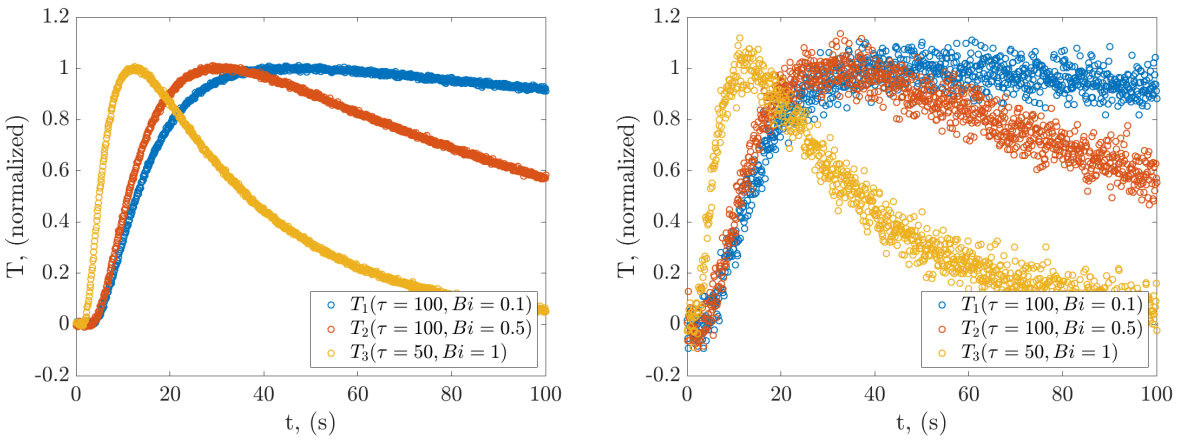

*Fig. 5: Normalized thermograms for the three different couples (τ, Bi) presented: **(a)** SNR = 200 and **(b)** SNR = 20.*

Generation of the numerical reference base

For the Bayesian method, a numerical base that contains the temperature of reference $T_r(t, \boldsymbol{\beta})$ is used in equation 10. According to the needs, this base can be calculated beforehand in

the form of an abacus or can be generated at the same time as the estimation. The only essential point of this base is that the time interval and the time discretization of thermograms in the base must be the same as those of the measured thermograms $T_m(t)$. Conversely, regarding the choice of the parameters $\boldsymbol{\beta}$, there are no real constraints for the base, except that it is recommended to have a sufficiently broad spectrum so that it can approach the real solution.

For the generation of the base, the idea is to use the Parker method to focus the Bayesian estimation around a first estimation τ_0 instead of searching in the whole range of existing parameters τ. For the example illustrated by figure 5, as it is supposed we have a better *a priori* knowledge for the diffusivity than for the heat loss thanks to the Parker method, the base is generated with 100 values of τ linearly distributed on the interval $[20, 200]$ and 100 values of Bi linearly distributed on the interval $[0, 2]$ to have 10000 different thermograms with a unique couple (τ, Bi). To understand the physical correspondence, for a sample of thickness $e = 1$ cm, τ varying from 20 to 200 corresponds to the diffusivity a varying on the interval $[0.5, 5] \times 10^{-6}$ $\text{m}^2\cdot\text{s}^{-1}$. Bi varies from 0 to 2 for a sample of conductivity $\lambda = 1$ $\text{W}\cdot\text{m}^{-1}\cdot\text{K}^{-1}$ (a PVC, for example), corresponds to the heat loss h ($\text{W}\cdot\text{m}^{-2}\cdot\text{K}^{-1}$) varying on the interval $[0, 200]$.
The complete calculation of such a base takes 5.1 s on a 2.3 GHz quad-core i7 laptop with 16 GHz of RAM.

Implementation of the estimation algorithm

The Bayesian method, as depicted in part 2.4, is then performed for each of the three thermograms and for each noise level, illustrated by figure 5 with the help of the generated base. For the three thermograms, the likelihoods are then computed from equation 10. The posterior probabilities are obtained for each couple (τ, Bi) of the base. The obtained repartition of posterior probabilities for the thermogram T_3 is presented in figure 6.a for the case with SNR $= 200$ (low noise level) and in figure 6.b for SNR $= 20$ (high noise level).

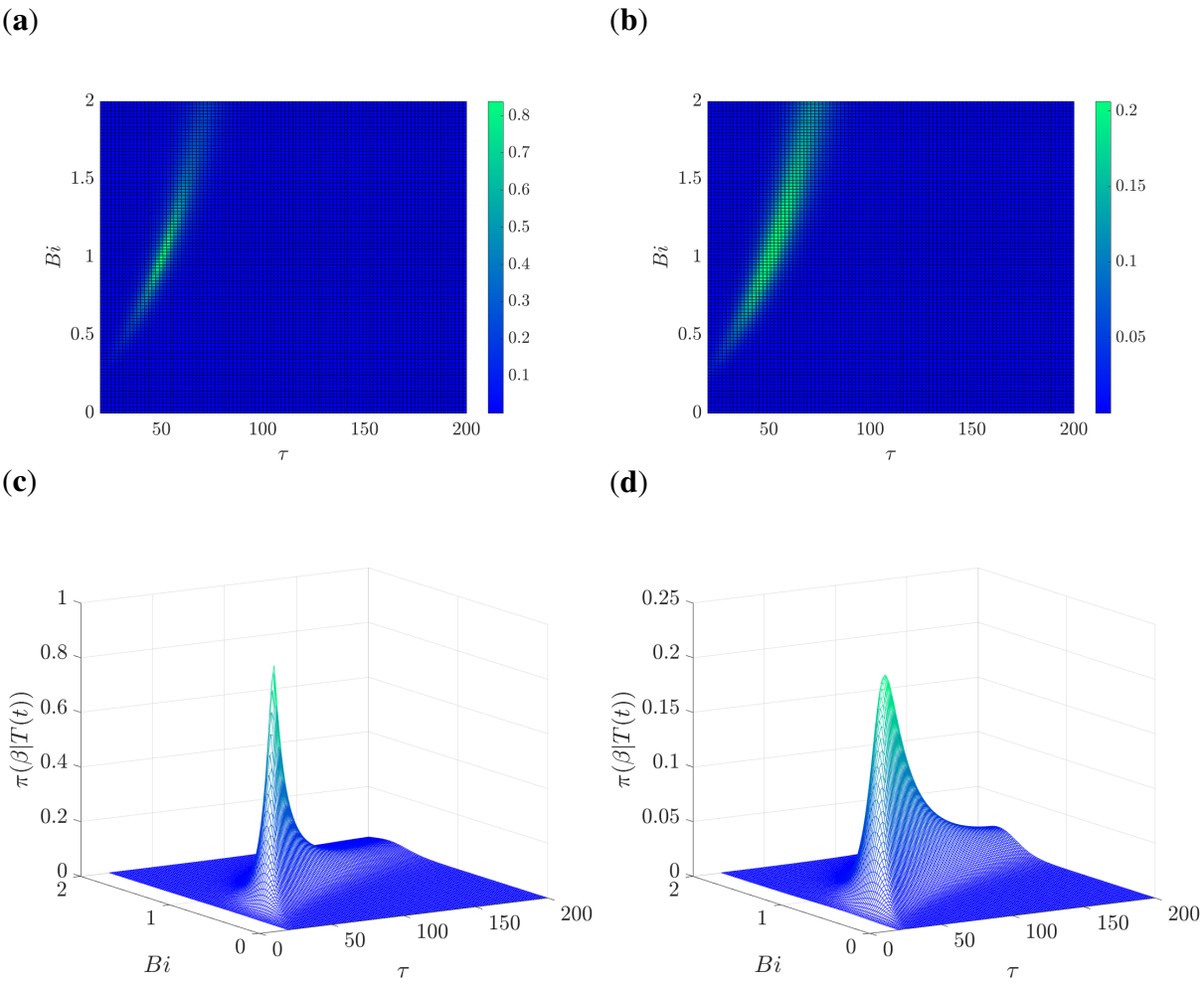

*Fig. 6: Posterior probabilities for the thermogram T_3 for each value of the β couple: Representation in image **(a)** for SNR = 200 and **(b)** for SNR = 20. Representation in 3D **(c)** for SNR = 200 and **(d)** for SNR = 20.*

The probabilities are higher for a low noise level (figure 6.a and figure 6.c) than for a high noise level (figure 6.b and figure 6.d); however, the form of the probability repartition is the same, and therefore, the position of the maximum of probabilities remains the same. This maximum probability corresponds to the best estimation of the couple of parameters (τ, Bi). The influence of noise level is therefore low. From the location of the maximum of the posterior probabilities, the corresponding couple of parameters can be extracted. For the 3 examples, the reconstructed temperatures with the estimated parameters are illustrated in figure 7 for the two distinct noise levels. For comparison, the estimation of the two parameters has been made in parallel with the Levenberg-Marquardt minimization method.

(a) **(b)**

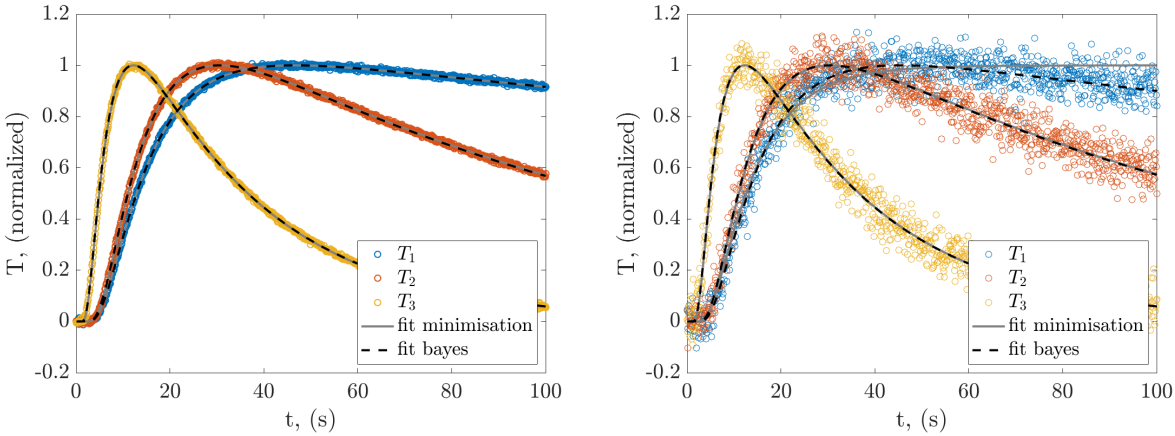

Fig. 7: Normalized thermal responses and their estimations with Bayesian inference and minimization: ***(a)*** *slightly noised temperature and* ***(b)*** *highly noised temperature.*

The reconstructed thermograms with the estimated parameters fit the measured thermograms with a very good accuracy, for any noise level, for the Bayesian method. However, for the high noise level, the minimization can lead to a bad estimation, as seen for the thermogram T_1. To compare the errors made by the two methods, a parametric study for large numbers of τ and Bi was performed for different noise levels.

3.2 Parametric study and noise influence

In this part, the two methods are performed for broad values of couples (τ, Bi) and for different noise levels. As in the previous part, the "real thermograms" are computed numerically, and white noise is added to simulate a real measure. Then, the estimation of the couple (τ, Bi) is made with the two methods (minimization and Bayesian). For the minimization, the initial conditions are given by Parker for τ, and Bi takes n equal to 1. This methodology is performed for each couple (τ, Bi), and the absolute error is calculated between the estimated and real parameters. The fields of errors are illustrated in figure 8 for each parameter and for the two methods for an SNR $= 20$.

For the minimization, for SNR $= 20$, there is a large area located for $\tau \in [60, 120]$ and for $Bi \in [0.1, 0.6]$ where the error is high, both for the τ and the Bi parameter. As shown in figure 8.a., the error is approximately 35% for the τ parameter, and in figure 8.c, it can be higher than 100% for the Bi parameter. For the Bayesian method, this area is not specific, and the errors are much lower: less than 5% for τ and less than 20%, as illustrated in figure 8.b and figure 8.d, respectively.

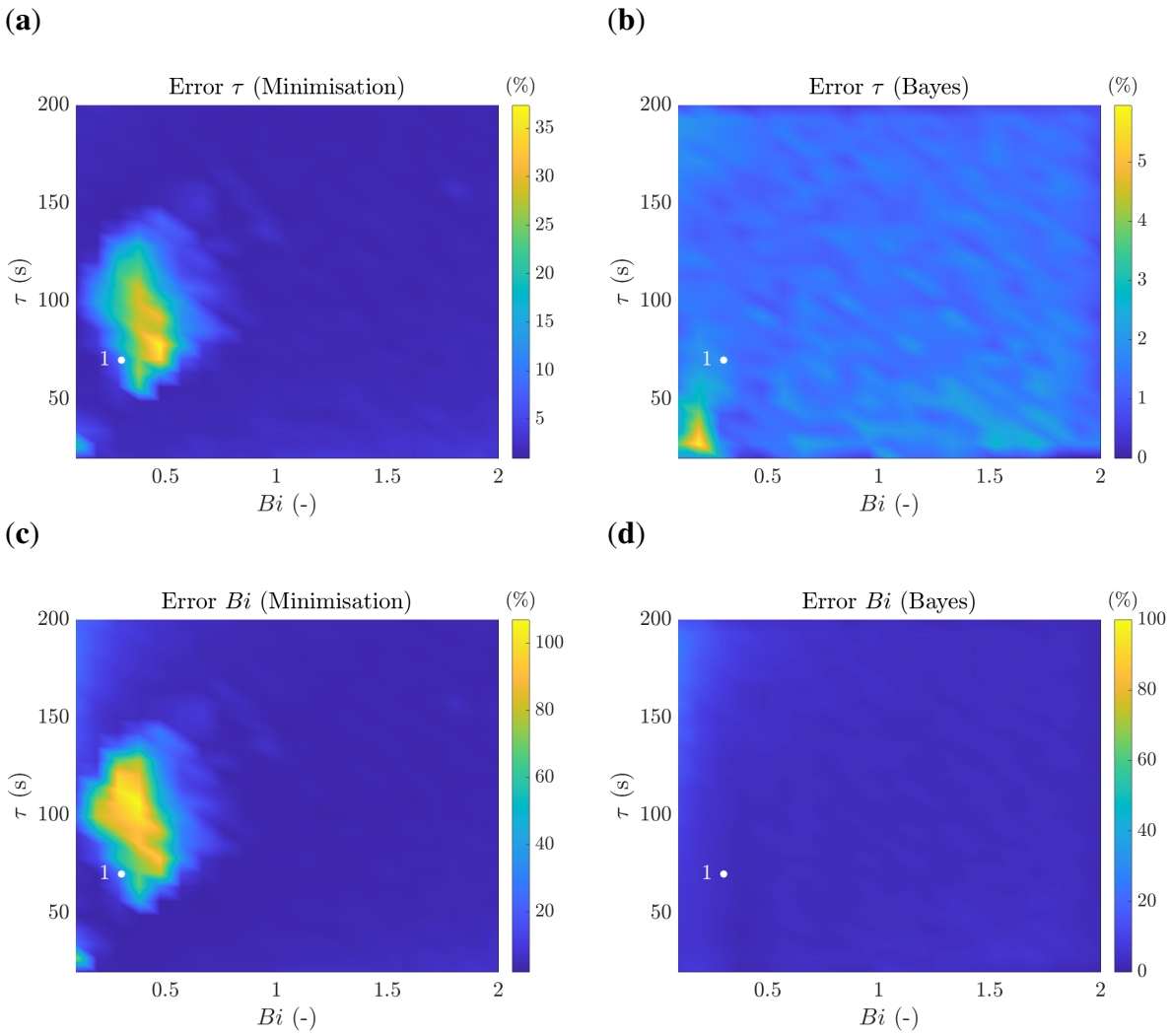

*Fig. 8: Fields of error estimations on the parameters τ and Bi for SNR = 10. Error on the estimation of τ with **a)** the minimization and **b)** the Bayesian method. Error on the estimation of Bi with **c)** the minimization and **d)** the Bayesian method.*

For the minimization method, this "area of error" is dependent on the initial condition of the minimization. The location of this area is indeed decaled for different initial conditions for Bi. Likewise, the intensity of the error is dependent on the SNR. To illustrate these results, the evolution of the error as a function of the SNR is presented in figure 9 for point 1, which is located in figure 8. This point corresponds to the couple (τ, Bi) = $(70, 0.3)$. For both methods, the error made on the τ parameter is represented with a continuous line, whereas the error made on Bi is represented with a dashed line. For the minimization method, the error decreases when the SNR increases.

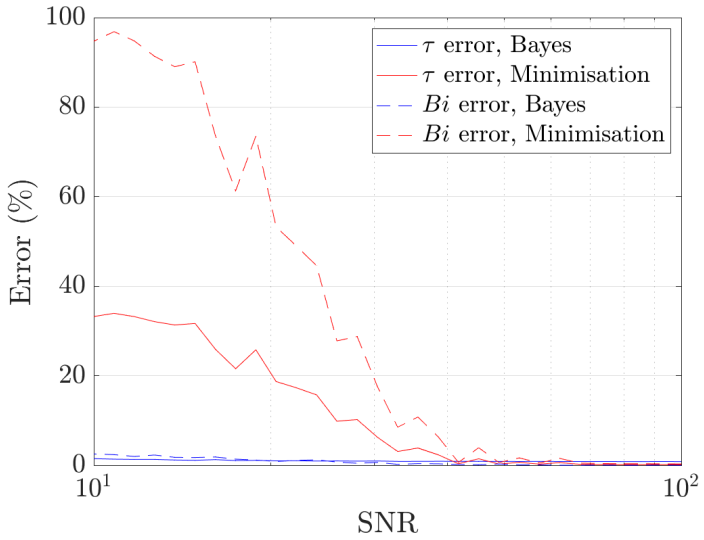

Fig. 9: Errors in the estimation of τ and Bi as a function of the SNR (logarithmic scale) for point 1 presented in figure 8.

For the Bayesian method, the errors are almost constant and almost independent of the noise level. For the Bayesian method, it is also important to note that the error depends on the chosen interval between two parameters of the generated base because it gives precision to the estimation. It can be noted that it is always possible to generate a second refined numerical base around the estimated couple (τ, Bi) to obtain a better estimation if needed, in the same manner as presented in [24].

Another point to discuss is the time computation of the algorithm. Once the base is generated, the Bayesian algorithm to perform the estimations on the three thermograms takes 0.07 s, whereas the LM algorithm takes 0.18 s. In this case, the difference is negligible, but for larger values of thermograms, the difference will be important, as will be presented in the next part.

Thus, the Bayesian method enables the estimation (τ, Bi) parameters with very good precision. This method is easy to implement and minimally sensitive to noise.

4 Experimental case on high insulated media

In this part, the results obtained on an experimental case are presented. The studied sample is composed of two juxtaposed materials of the same thickness $e = 3$ mm but different diffusivities: a PVC and a foam, as illustrated by figure 10. The theoretical values of diffusivity for the PVC is around 2×10^{-7} m^2·s^{-1} whereas it is 1.5×10^{-7} m^2·s^{-1} for the Foam. The objective is to determine the parameters τ and Bi on each pixel of the surface. In this example, a foam and a PVC were chosen because the thermal conductivity for an insulator (foam) tends toward zero,

and therefore, the Biot number increases. The ratio between the two Biot numbers will enable the estimation of the thermal conductivity of the foam, as will be presented at the end of this part.

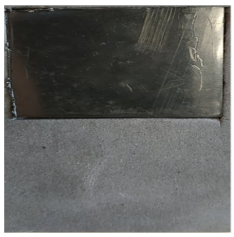

Fig. 10: Photography of the studied material.

The experimental setup used for this example is presented in part 2.1. The study was focused on the sample on a rectangle of dimensions 8×7 cm^2, with a resolution of 280 μm^2 per pixel. The camera frequency rate was fixed to 10 Hz, and the final acquisition time was fixed at 60 s.

On each pixel, a first estimation τ_0 is made with the Parker method, and the obtained results are illustrated in figure 11. For both materials, the estimations are similar, $\tau \approx 40$ s at each pixel.

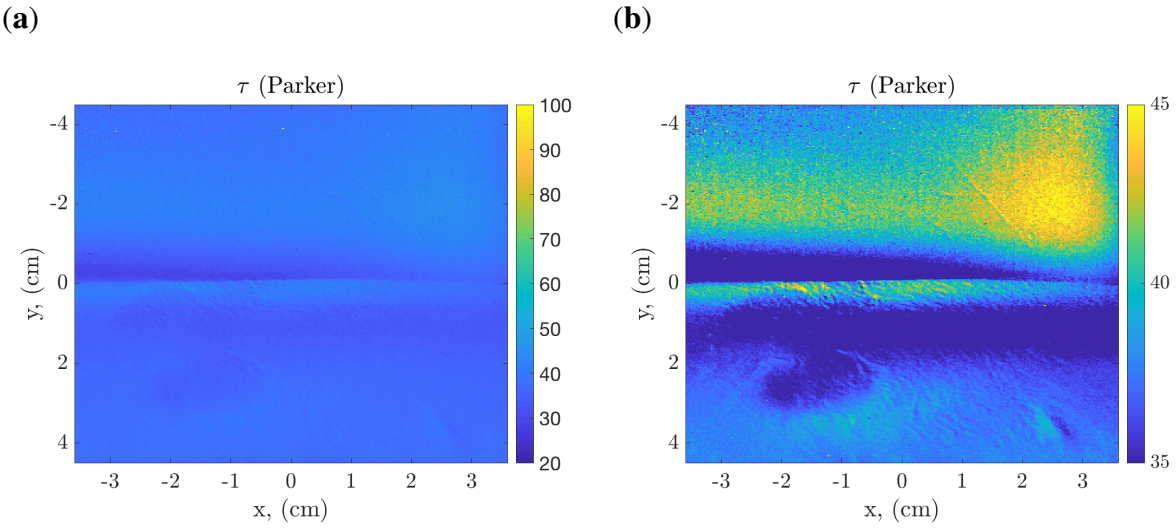

*Fig. 11: Estimation of the parameters τ on each pixel of the sample with the Parker method: **a)** with a scale between 20 and 100 and **b)** with a scale centered at approximately 40.*

The distinctive line that can be seen in figure 11 at $y = 0$, where the τ estimation seems lower, is an artefact because the junction between the two materials (foam + PVC) was not perfect.

Then, to perform the Bayesian methodology, the implementation on a base, as depicted in part 2.4, is performed. For this example, the base is generated with 50 values of τ linearly distributed on the interval $[20, 100]$ (which is around the value $\tau = 40$ estimated with the Parker

method) and 30 values of Bi logarithmically distributed on the interval $[0, 6]$, which leads to 1500 different thermograms with a unique couple (τ, Bi). The calculation of this base takes 2 s.

The estimation of the couple (τ, Bi) is then performed on each pixel with the Bayesian methodology. In parallel, the same estimation is performed with an inversion with the LM algorithm, where the initial values for τ at each pixel are the values given by the Parker method. The results are given by figure 12. Figure 12.a and Figure 12.b illustrate the τ parameters with the minimization and Bayesian methodology, respectively, and Figure 12.c and Figure 12d. the estimation of Biot number.

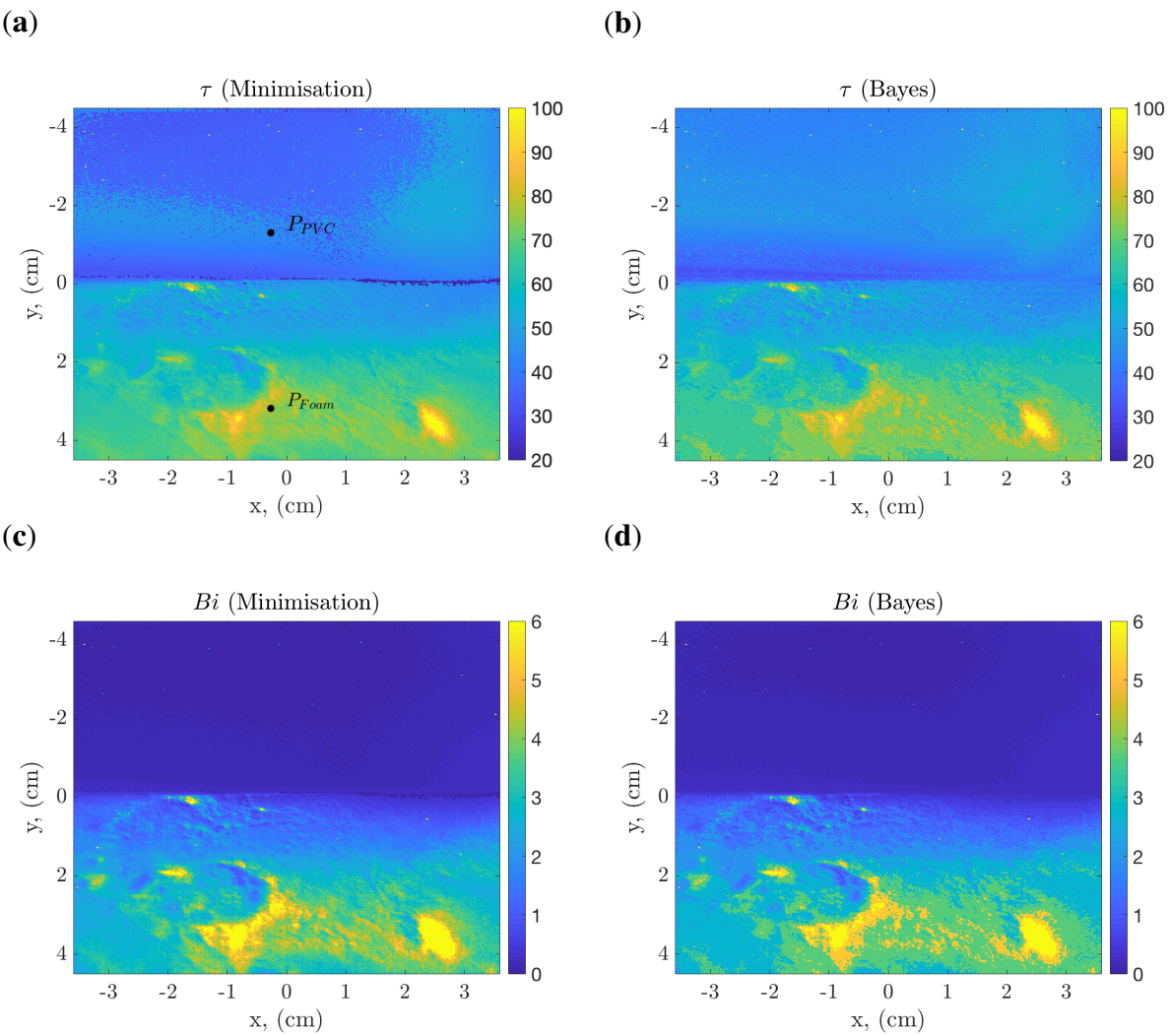

*Fig. 12: Estimation of the parameters τ on each pixel of the experimental material by **a)** minimization with the LM algorithm and **b)** Bayesian method. Estimation of the adimensional Biot number Bi on each pixel of the sample with **c)** minimization and **d)** Bayesian method.*

It can be observed that the results on the estimations for the couple (τ, Bi) are very similar for the two different methods of estimation. The depth of each material is 3 mm, then the estima-

tion of the thermal diffusivity can be made on each point with equation 3. The average value of the diffusivity is 1.99×10^{-7} m^2·s^{-1} for the PVC and for the foam it is 1.47×10^{-7} m^2·s^{-1} which are consistent with the theoretical values.

To evaluate the accuracy of the estimation, the focus is on points P_{PVC} and P_{Foam} of the sample, the first one on the PVC and the second on the foam, represented in figure 12.a. The thermograms measured by the IR camera are illustrated in figure 13 as well as their fit with the estimated (τ, Bi) for both the minimization and the Bayesian methodology. The estimation of the τ parameter with the Parker method and the reconstructed parameter is also presented.

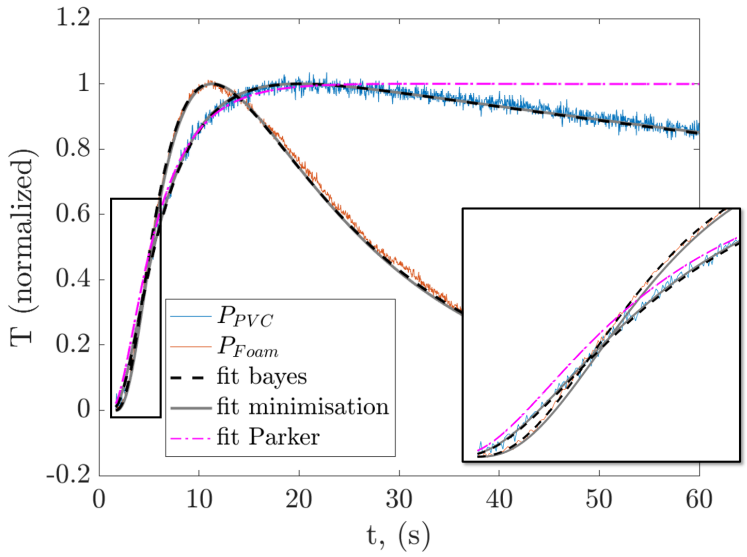

Fig. 13: Measured thermograms at pixels P_{PVC} and P_{Foam} of figure 12.a and their fit with the Bayesian method and with LM minimization.

The Parker estimation leads to the same value of τ for the two pixels (PVC and Foam). The two resulting thermograms are then superposed and do not fit the measured thermograms, even during the rising time of temperature, as shown in figure 13. These results are consistent with the conclusion drawn by part 2.3. Figure 13 shows that the estimation of the couple (τ, Bi) is better with the Bayesian method than with the LM minimization because the reconstructed thermograms with the estimated parameters fit the measured thermograms with better accuracy.

Moreover, the high difference between the two methods is the computation time: the complete estimation of the couple (τ, Bi) on each pixel of the sample was taking at 2 h 35 min for the LM algorithm, whereas it was only 20 min with the Bayesian methodology, with similar precision. This difference is explained by the type of algorithm. Minimization methods such as the LM algorithm require the inversion of matrices, which is of high complexity, whereas Bayesian methodology is based on the subtraction of thermograms, which is of minimal complexity.

Relative estimation of the thermal conductivity

The Biot number is dependent on the heat loss h, the thickness e and the thermal conductivity λ of the studied material. In the previous experiment, the thickness e was the same for the PVC and the foam. The two materials were placed in the same environment; therefore, the heat loss coefficient h can be assumed to be identical. Then, the ratio between the Biot numbers leads to the ratio between the thermal conductivity of the two materials, as presented by equation 11:

$$\frac{Bi_{Foam}}{Bi_{PVC}} = \frac{\lambda_{PVC}}{\lambda_{Foam}} \tag{11}$$

Thus, the estimation of the couples (τ, Bi) for two juxtaposed materials enables a ratio between the thermal conductivities of these two materials. If the conductivity of one of the materials is known, the second conductivity can then be estimated.

The ratio between the Biot numbers and the mean Biot number of the PVC is determined on the results obtained in figure 12.d and illustrated in figure 14. The mean value of Bi_{PVC} is 0.11 in this example.

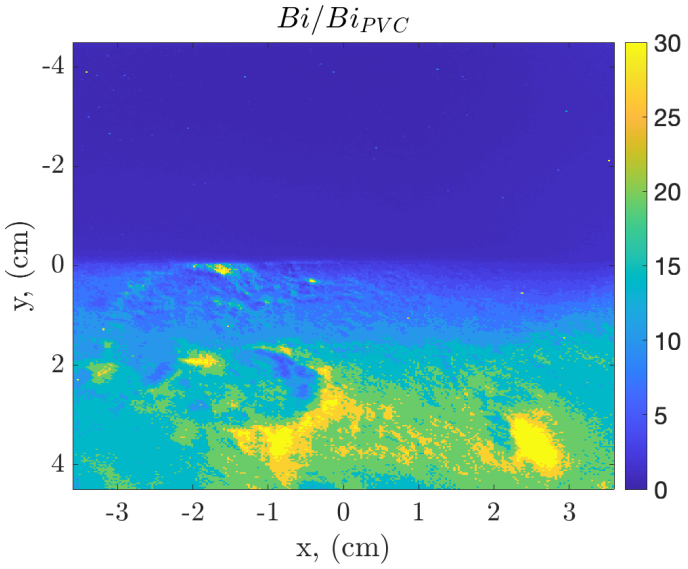

Fig. 14: Ratio between the Biot numbers of the Foam and the mean Biot numbers of the PVC leading to the ratio values of the thermal conductivity between the two materials.

The mean Biot number ratio obtained for the foam is 26.9, which means that the thermal conductivity of the PVC is 26.9 times greater than the thermal conductivity of the foam. This result is consistent with the materials used; the thermal conductivity of a PVC is approximately 10^{-1} W.m^{-1}. K^{-1}, whereas the foam used is approximately 2-3$\times 10^{-2}$ W.m^{-1}.K^{-1}. This setup can then be used as a first estimation method for the thermal conductivity of any material in addition to the thermal diffusivity. This methodology can be compared to the hot disk transient plane source (TPS) methods [25, 26, 27] that allow the estimation of the thermal conductivity,

the thermal diffusivity and the specific heat capacity in a single measurement. Conductivity and diffusivity are tested directly, and specific heat is calculated from the former two.

5 Conclusion

A method based on Bayesian inference was proposed to conjointly estimate the following two fields of thermophysical parameters: a thermal characteristic time τ directly linked to the thermal diffusivity and the thickness and the Biot number, directly linked to the heat loss and the thermal conductivity. This method is robust to noise and leads to very good estimations of the parameters, with results comparable to a classical minimization method. This method is, however, very fast and less time consuming. A setup and methodology are also presented to estimate the average value of the thermal conductivity of an unknown material.

Author declarations

Conflict of interest

The authors have no conflicts to disclose.

Data availability

The data that support the findings of this study are available from the corresponding author upon reasonable request.

References

[1] Parker, W., Jenkins, R., Butler, C. & Abbott, G. Flash method of determining thermal diffusivity, heat capacity, and thermal conductivity. *Journal of Applied Physics* **32**, 1679–1684 (1961). 2, 5, 6

[2] Balageas, D. Flash thermal diffusivity measurements using a novel temperature-time history analysis. *ONERA* **1981** (1981). 2

[3] Degiovanni, A. *et al.* Diffusivite et methode flash. (1977). 2

[4] Degiovanni, A. Diffusivity and flash method. *Revue Générale de Thermique* **16**, 420–442 (1977). 2

[5] Degiovanni, A., Sinicki, G. & Laurent, M. Heat pulse thermal diffusivity measurements-thermal properties temperature dependence and non-uniformity of the pulse heating. In *Thermal Conductivity 18*, 537–551 (Springer, 1985). 2

[6] Degiovanni, A. & Laurent, M. Une nouvelle technique d'identification de la diffusivité thermique pour la méthode «flash». *Revue de physique Appliquée* **21**, 229–237 (1986). 2

[7] Mourand, D., Gounot, J. & Batsale, J.-C. New sequential method to process noisy temperature response from flash experiment measured by infrared camera. *Review of scientific instruments* **69**, 1437–1440 (1998). 2

[8] Takahashi, Y., Yamamoto, K., Ohsato, T. & Terai, T. Usefulness of logarithmic method in laser-flash technique for thermal diffusivity measurement. In *Proc. 9th Japan Symp. Thermophysical Properties*, 175–178 (1988). 2

[9] Hohenauer, W. & Vozar, L. Flash method of measuring the thermal diffusivity. *High Temp.–High Pressures* **35**, 253–264 (2003). 2

[10] Pawlowski, L. & Fauchais, P. The least square method in the determination of thermal diffusivity using a flash method. *Revue de physique appliquée* **21**, 83–86 (1986). 2

[11] Sheindlin, M., Halton, D., Musella, M. & Ronchi, C. Advances in the use of laser-flash techniques for thermal diffusivity measurement. *Review of scientific instruments* **69**, 1426–1436 (1998). 2

[12] Chihab, Y., Garoum, M. & Laaroussi, N. A new efficient formula for the thermal diffusivity estimation from the flash method taking into account heat losses in rear and front faces. *International Journal of Thermophysics* **41**, 1–27 (2020). 2

[13] Chihab, Y., Raefat, S., Garoum, M., Laaroussi, N. & Bouferra, R. Numerical inverse estimation of the thermal diffusivity and the adiabatic limit temperature of three types of unfired clay bricks using flash method and global minimization algorithm. In *IOP Conference Series: Materials Science and Engineering*, vol. 446, 012008 (IOP Publishing, 2018). 2

[14] Fudym, O., Orlande, H. R. B., Bamford, M. & Batsale, J. C. Bayesian approach for thermal diffusivity mapping from infrared images with spatially random heat pulse heating. In *Journal of Physics: Conference Series*, vol. 135, 012042 (IOP Publishing, 2008). 2

[15] Berger, J., Orlande, H. R., Mendes, N. & Guernouti, S. Bayesian inference for estimating thermal properties of a historic building wall. *Building and Environment* **106**, 327–339 (2016). 2

[16] Maillet, D. *Thermal quadrupoles: solving the heat equation through integral transforms* (John Wiley & Sons Inc, 2000). 4

[17] Stehfest, H. Algorithm 368: Numerical inversion of laplace transforms [d5]. *Communications of the ACM* **13**, 47–49 (1970). 4

[18] Moré, J. J. The levenberg-marquardt algorithm: implementation and theory. In *Numerical analysis*, 105–116 (Springer, 1978). 7

[19] Bayes, T. An essay towards solving a problem in the doctrine of chances. 1763. *MD computing: computers in medical practice* **8**, 157 (1991). 8

[20] Kaipio, J. & Somersalo, E. *Statistical and computational inverse problems*, vol. 160, 49–112 (Springer Science & Business Media, 2006). 8, 9

[21] Carlin, B. P. & Chib, S. Bayesian model choice via markov chain monte carlo methods. *Journal of the Royal Statistical Society: Series B (Methodological)* **57**, 473–484 (1995). 9

[22] Metropolis, N., Rosenbluth, A. W., Rosenbluth, M. N., Teller, A. H. & Teller, E. Equation of state calculations by fast computing machines. *The journal of chemical physics* **21**, 1087–1092 (1953). 9

[23] Derin, H., Elliott, H., Cristi, R. & Geman, D. Bayes smoothing algorithms for segmentation of binary images modeled by markov random fields. *IEEE Transactions on Pattern Analysis and Machine Intelligence* 707–720 (1984). 9

[24] Groz, M. *et al.* Thermal resistance field estimations from ir thermography using multiscale bayesian inference. *Quantitative InfraRed Thermography Journal* 1–12 (2020). 14

[25] Gustafsson, S. E. Transient plane source techniques for thermal conductivity and thermal diffusivity measurements of solid materials. *Review of scientific instruments* **62**, 797–804 (1991). 18

[26] Gustavsson, M., Karawacki, E. & Gustafsson, S. E. Thermal conductivity, thermal diffusivity, and specific heat of thin samples from transient measurements with hot disk sensors. *Review of Scientific Instruments* **65**, 3856–3859 (1994). 18

[27] Gustavsson, M., Saxena, N., Karawacki, E. & Gustafsson, S. Disk thermal constants analyser. *Thermal Conductivity 23* **23**, 56 (1996). 18